A DIFFUSIONLESS TRANSFORMATION PATH RELATING Th_3P_4 AND SPINEL STRUCTURE

OPPORTUNITIES TO SYNTHESIZE CERAMIC

MATERIALS AT HIGH PRESSURES

by

ARINDOM GOSWAMI

Presented to the Faculty of the Graduate School of

The University of Texas at Arlington in Partial Fulfillment

of the Requirements

for the Degree of

MASTER OF SCIENCE IN CHEMISTRY

THE UNIVERSITY OF TEXAS AT ARLINGTON

AUGUST 2011

ACKNOWLEDGEMENTS

There are so many people I am thankful to without whom this thesis would not be possible. First and foremost, I am thankful to my supervising professor Dr. Peter Kroll for taking me under his wings and constantly motivating and encouraging me to thrive towards my goal, and also for taking the time to critically evaluate this manuscript.

I wish to thank my former academic advisor Dr. Zoltan Schelly, and special thanks to Dr. Krishnan Rajeswar and Dr. Richard Timmons for their interest in my research and for taking time to serve in my dissertation committee.

I wish to thank all my lab-mates Babak Kouchmesky, Munuve Mwania, Ibukun Olubanjo and Nelli Klinova for their keen interest in all my work and for helping me with their inputs/comments and constructive criticism. I wish also to thank my roommates and all the friends from UTA and UT southwestern for their support and encouragement. I am grateful to all the teachers who taught me during the years I spent in school, first in India, and finally in the Unites States.

Last but not the least, I would like to express my deep gratitude to my family who have encouraged and inspired me and supported me throughout my undergraduate and graduate studies. I am also extremely grateful to them for their sacrifice, patience and for being there for me during all my highs and lows.

July 28, 2011

ABSTRACT

A DIFFUSIONLESS TRANSFORMATION PATH RELATING Th_3P_4 AND SPINEL STRUCTURE:OPPORTUNITIES TO SYNTHESIZE METASTABLE CERAMIC MATERIALS AT HIGH PRESSURES

Arindom Goswami, M.S.

The University of Texas at Arlington, 2011

Supervising Professor: Peter Kroll

Physical properties of solids at high pressure hold the key to many interesting questions in earth and planetary sciences, as well as in applied sciences. At high pressure, most ambient-pressure materials become unstable and transform into new and denser phases. In recent years, many solids with new structure types have been realized at high pressure through experiments and predicted in numerical simulations. Some of these structures are novel and had not been seen at ambient pressure. Some possess a variety of electronic states, i.e., metallic, superconducting, or super-hard states [YAO08]. These discoveries are of high interests both for their potential technological applications and contribute to the understanding of the fundamental aspects of electronic processes in solids such as chemical bonding. The study of physical properties of high-pressure solids is one research area that have greatly benefited from computational research. In experiments, high pressure can be attained, for instance, in diamond anvil cells. Adjusting pressure in computational studies can be accomplished straightforwardly by varying the size of unit cell. With the rapid developments of

computational power and advanced software, theoretical studies of solids at high pressure bloom over the past two decades. The complexities of the materials that can be studied and the accuracy in which physical properties can be predicted have increased rapidly over the years. Computations with well-established first-principles methods have played an important role in exploring and guiding experiments at high pressure. Numerical simulations have now been established as an important tool in cooperation with experiments at high pressure. On the other hand, new experiments at high pressure continue to provide challenging tests for both theory and numerical methods, and help to further develop more sophisticated principles and algorithms [MON07].

TABLE OF CONTENTS

ACKNOWLEDGEMENTS iii

ABSTRACT iv

LIST OF ILLUSTRATIONS viii

LIST OF TABLES ix

Chapter Page

1. INTRODUCTION 1

1.1 High Pressure Chemistry of Novel Compounds 1

1.2 Nitrides 1

1.2.1 Group 4 transition metal nitrides 2

1.3 Goal of this work 4

2. METHODOLOGY 6

2.1 Density Functional Theory (DFT) 6

2.1.1 VASP (Vienna Ab-initio Simulation Package) 6

2.2 Computational approach 7

3. INTRODUCTION TO THE TRANSFORMATION PATH 8

3.1 The Bain Correspondence 8

3.2 Description of the structures: the spinel structure (fcc) and its bcc counterpart Th_3P_4 type 9

3.3 Crystallographic description of the transformation path 10

4. RESULTS 12

4.1 Variation of energy and enthalpy under pressure 12

4.2 Energy profile calculation along the reaction coordinate 14

4.2.1 Results of energy profile calculation 16

5. SUMMARY AND CONCLUSION 18

REFERENCES 19

BIOGRAPHICAL INFORMATION 21

LIST OF ILLUSTRATIONS

Figure Page

1 Goal of this work 4

2 The Bain Correspondence 8

3 Spinel structure 9

4 Th_3P_4 structure: a) cation position and b) anion position 10

5 Energy-volume (E-V) (up) and enthalpy-pressure (ΔH-p) diagrams (down) of Hf_3N_4 13

6 Energy-volume (E-V) (up) and enthalpy-pressure (ΔH-p) diagrams (down) of Ti_3N_4 14

7 Energy profile diagram along the reaction coordinate for Hf_3N_4 15

8 Energy profile diagram along the reaction coordinate for Ti_3N_4 15

9 Enthalpy profile diagram along the reaction coordinate for Ti_3N_4 16

10 Enthalpy profile diagram along the reaction coordinate for Hf_3N_4 17

LIST OF TABLES

Table Page

1 Crystallographic description of the transformation path 11

2 Structure type, energy E_0 and volume V_0 calculated at zero pressure, relative energy ΔE with respect to the ground state configuration for the three polymorphs of interest of Hf_3N_4 13

3 Structure type, energy E_0 and volume V_0 calculated at zero pressure, relative energy ΔE with respect to the ground state configuration for the three polymorphs of interest of Ti_3N_4 14

CHAPTER 1

INTRODUCTION

1.1 High Pressure Chemistry of Novel Compounds

Under high-pressure conditions, chemical reactivity of atoms and molecules increases manifold, significant shift in chemical equilibria observed and reaction rates get affected. On compression of any substance, distances between constituting atoms decrease and its electronic structure deforms. This leads to increase of the internal energy of the substance, and formation of denser structures could become energetically favorable on further compression [KOS01]. Shorter interatomic distances and/or higher coordination numbers of the constituent atoms characterize such structures when compared with the lower pressure phases. At high-pressure conditions, formation of compounds with elements in unusual oxidation states can take place. In many cases, these high-pressure phases can be quenched to ambient conditions where they may persist metastably due to slow kinetics of a reverse transformation [BOL09]. Such metastable products can have a number of unique physical and chemical properties, from high hardness and corrosion stability to interesting optoelectronic, magnetic or superconducting properties. Therefore, they can be of potential interest for various industrial applications.

1.2 Nitrides

Nitrides have found extensive use in industry because of their unique physical, chemical, electrical, optical or mechanical properties. The high pressure cubic phase of boron nitride, c-BN is the second hardest material after diamond. AlN, GaN and InN all have interesting semiconductor properties, and each one of them possesses a NaCl-type high pressure phase. Nitrides are used for different applications as refractory ceramics (hexagonal BN, α- and β-Si_3N_4, AlN, TiN), hard grinding materials (cubic BN, α- and β-Si_3N_4), in light emitting diodes (GaN, InN), as catalysts (Mo_2N, W_2N), sintering additives, and as electrolyte in

lithium batteries (Li_3N) [DZI09]. Recent progress in the study of nitrides is mainly due to development of new synthetic routes, which allows large production of compounds and also leads to the discovery of novel compounds [MON07].

Discovery of a new family of high-pressure group 14 cubic spinel nitrides, γ-A_3N_4 (A=Si, Ge or Sn) [ZER99] is partially responsible for the upsurge in the interest in the high-pressure nitrides during the last decade. γ-Si_3N_4, in particular, has unique combination of hardness and stability (both thermal as well as oxidation) and also a wide band gap semiconductor, which can be used in fabrication of blue LEDs.

Another particular family of ceramics are nitrides of the group 4 elements. High-pressure and high-temperature experiments with transition metals of group 4 resulted in the discovery of exotic family of high-pressure nitrides, c-Zr_3N_4 and c-Hf_3N_4, with cubic Th3P4-type structure [ZER03].

Since this thesis deals and investigates structural relations among high pressure phases of group 4 elements, we briefly discuss synthesis methods, structure, and experimental and theoretical studies of recently discovered high-pressure zirconium (IV)- and hafnium (IV) nitrides in the following section.

1.2.1 Group 4 transition metal nitrides

At ambient pressure conditions, mononitrides of group 4 transition metals having a cubic rocksalt structure type exist. These mononitrides can also be specified as δ-MN (M= Ti, Zr or Hf). They are used as refractory materials, and as coatings over tools as wear resistant layers. Although they are brittle and hard in comparison to other transition metals, they still exhibit metallic character. All the three mononitrides show superconducting properties with relatively high critical temperatures of 5.8, 10.5 and 6.9 K for TiN, ZrN and HfN, respectively [LEN00]. One more interesting property of these nitrides is their defect structure. They can form several non-stoichiometric structures by creating vacancies on the corresponding lattice sites while still maintaining NaCl-type structure. As for example, in δ-HfN_x, x can have values from 0.74 to 1.7

and in δ-ZrN_x, x can vary from 0.54 to 1.35 [KRA98]. Presence of vacancies affect their properties significantly. When x > 1, δ-HfN_x and δ-ZrN_x can transform to insulating phases from metallic phases with an increase in nitrogen content. δ-TiN_x maintains its metallic character for all the known compositions [AND97].

Out of all the stoichiometric M_3N_4 compounds of group 4 transition metals, only orthorhombic zirconium (IV) nitride, o-Zr_3N_4 was known for long [LER96]. The o-Zr_3N_4 was found to be insulating and diamagnetic. It decomposes above 1100 K on heating in presence of nitrogen yielding δ-ZrN and N_2. It oxidizes in air at 800 K [LER97]. The high-pressure investigation of group 4 transition metal nitrides of the type A_3N_4 was an extension of study of spinel nitrides. Discovery of novel γ-A_3N_4 (A=Si, Ge or Sn) has set the trend of investigation of possible existence of stable spinel nitrides of similar tetravalent elements like group 4 transition metals. On performing experiment at high temperature and pressure, treating Ti, Zr and Hf (or their mononitrides) with molecular nitrogen in a LH-DAC, Zr_3N_4 and Hf_3N_4 with cubic Th_3P_4 structure type results (for Zr-N system at 15.8-18 GPa and 2500-3000 K and for Hf-N system at 18 GPa and 2800 K) [ZER03]. However, for Ti-N systems no other phase besides δ-TiN was observed in the pressure range 17.5-25 GPa and temperature ranging from 1500 to 3000 K. Examining the structure and surface morphology using XRD and EDX proved that the resulting structures are Zr_3N_4 and Hf_3N_4 with cubic Th_3P_4 structure type [ZER03]. The cubic Th_3P_4 structure type has cations eight-fold coordinated by nitrogen atoms, while nitrogens are six-fold coordinated by metal atoms (discussed in chapter 3). As the cation coordination number is higher (eight-fold) than NaCl-type mononitrides and o- Zr_3N_4 (six-fold) as well as in the hypothetical spinel nitrides (four- and six-fold), the density of c- Zr_3N_4 is 13% higher than o-Zr_3N_4. c-Zr_3N_4 and o- Hf_3N_4 are binary nitrides, first of its kind, with such high coordination number [ZER03]. Theoretical studies on their electronic properties followed after, which also supported structural assignment and low compressibility of c-M_3N_4 [KRO03b] as suggested by experiments. Theoretical work on nitrogen rich part of Ti-N, Zr-N and Hf-N P-T phase diagrams

provides equilibria conditions between δ-MN + N_2 and c-M_3N_4 phases [KRO04]. Interest on these materials increased rapidly with the recent finding that thin films made of c-Zr_3N_4 are significantly harder than those of δ-ZrN. Also, it functions as a better wear resistance tool in low-carbon steel manufacturing machine compared to δ-TiN [CHH05], which is a well-known wear resistant material. To sum up, the recently discovered cubic Zr_3N_4 and Hf_3N_4 are of utmost interest for use in industry for their microelectronics and wear-resistant applications.

1.3 Goal of this work

This work exploits a structural relation between the Th_3P_4-type, the structure type of novel high-pressure Hf_3N_4 and Zr_3N_4 and the spinel type. We will construct a transition path from Th_3P_4 to spinel phase. While the spinel type has not been observed among the group 4 transition metal nitrides, it is the target of this work to investigate under which conditions it may form from the existing Th_3P_4 –type. We, thus, will follow in two directions, which mark the goals of this work.

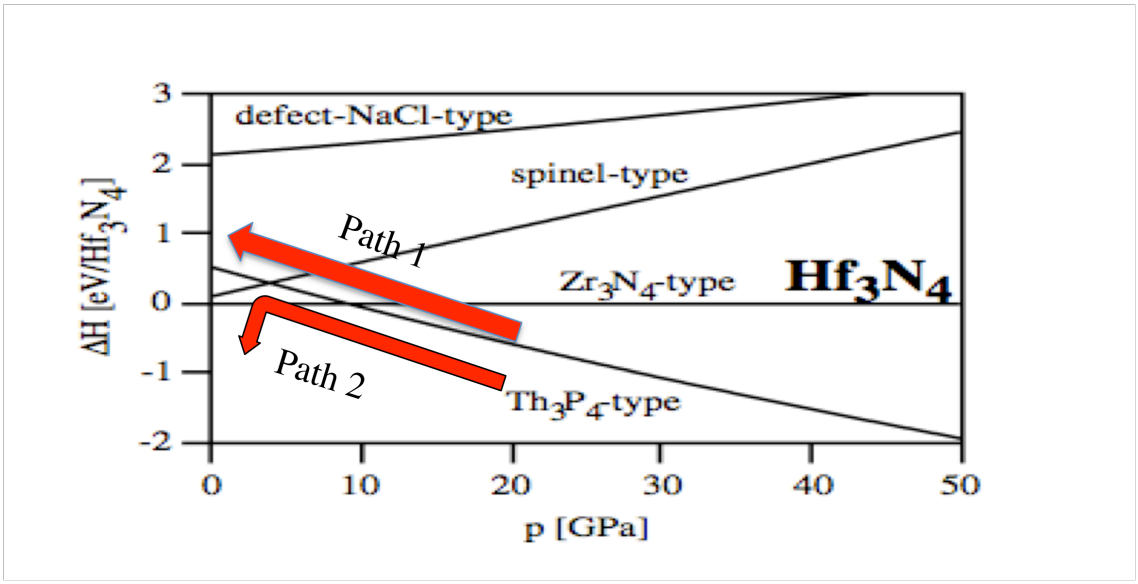

Figure 1: Goal of this work

First, we will compute the energy along the path from Th_3P_4 to spinel at ambient pressure. The resulting energy profile with its activation barrier will yield information about the thermal stability

of the Th_3P_4 type at ambient pressure. Second, we will repeat these calculations along the path at the transition pressure of the Th_3P_4-spinel transition. Since the enthalpy of both structures at this pressure is equivalent, a transformation will not yield excess energy. Therefore, the activation barrier will yield information about the temperature needed to activate the Th_3P_4-spinel transition.

CHAPTER 2

METHODOLOGY

2.1 Density Functional Theory (DFT)

Electrons and atomic nuclei constitute any solid material. The laws of quantum mechanics govern their properties. In principle, physical properties in a solid can be calculated by solving the many-body Schrodinger equation. Density functional theory (DFT) is the quantum mechanical approach used to solve the many-body Schrodinger equation. Electron density is the fundamental quantity in DFT. Electronic density replaces the complicated many-electron wave function, Ψ for efficient calculation of the Schrodinger equation, made possible by DFT.

Density functional theory (DFT) was introduced in 1960's by Hohenberg and Kohn [HOH64] and Kohn and Sham [KOH65]. The major breakthrough that came out from these two approaches are: a) ground-state energy can be written as a unique functional of the electron density [Hohenberg-Kohn] and b) introduction of an energy functional for the total energy of the electronic system to derive Schrodinger-like single-particle equations [Kohn-Sham]. DFT is very effective in computing electronic structure of materials. DFT is used to make predictions of several material properties such as structure, vibrational frequencies, elasticity coefficients, electronic and magnetic properties, paths in catalytic reactions, etc [CUE03]. Out of the many programs available for solid state calculations we have chosen the VASP (Vienna Ab-initio Simulation Package)-code, since it allows efficient and fast calculations.

2.1.1. VASP (Vienna Ab-initio Simulation Package)

VASP is used to perform first-principles electronic calculations. VASP implements the DFT combining a plane-wave basis set with the total energy pseudopotential approach. The pseudopotentials used are based on the Projector-Augmented-Wave (PAW) method

[KRE1999]. The PAW potential, in principle, is an all– electron potential and therefore allows the calculation all-electron properties.

The Generalized-Gradient Approximation (GGA) is used to treat the exchange-correlation energy of the electrons. Preferring the GGA over the Local Density Approximation (LDA) is based on the fact that gradient corrections yield more accurate results for the energy when comparing atoms in different environment. GGA reproduces experimental transition pressures while LDA artificially favors higher coordinated structures. All our results are obtained from well-converged structures with respect to cutoff energy (500 eV for nitrides and oxides) and k-point sampling.

2.2 Computational approach

While searching for new high-pressure modifications, the approach involves computations for structures from crystal database library. In a first step, a selected structure type is optimized in atomic positions and lattice parameters. Comparing the energies of various candidate structures the lowest energy modification for a compound is determined and, its energy and volume can be compared with all the other structure types [HOR06]. In a second step, the energy E is calculated for a series of volumes around the minimum energy structure for each candidate. The resulting energy-volume (E-V) data is used to calculate the enthalpy-pressure state function. The pressure p can be extracted from the E-V data by numerical differentiation. Using $p=- \delta E/\delta V$ the enthalpy $H= E + pV$ is obtained. Though it is the Gibbs energy, which determines thermodynamic stability, we neglect entropy contribution - $T\Delta S$ to the enthalpy. This approach is justified for compact compounds without sources of significant disorder, since entropy contributions $-T\Delta S$ are typically small in comparison to changes in relative enthalpy ΔH within a few GPa of pressure. Thus, comparing the enthalpy-pressure state functions for different structure types provides the structure with lowest enthalpy at a given p. The best way to extract the transformation pressure is to plot the enthalpy difference with reference to a reference state, usually the ground state.

CHAPTER 3

INTRODUCTION TO THE TRANSFORMATION PATH

3.1 The Bain Correspondence

bcc and fcc structures are related to each other by a tetragonal strain, either compression or extension. The mechanism governing the relation between these two structures is known as the Bain Correspondence. The bcc structure has a c/a ratio equal to 1. There is compression along the z-axis and a uniform expansion along the x and y axes resulting in change in c/a ratio to $\sqrt{2}$ in the resulting fcc structure [KRO03], [KIB07].

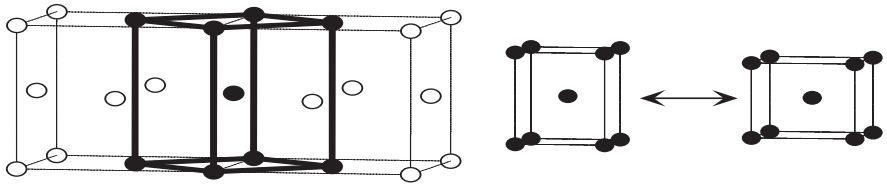

Figure 2: (Left) two unit fcc cells with a smaller body centered tetragonal cell marked in the center. By a homogeneous compression in the direction of arrows and an expansion in the plane normal to it, the bcc structure (right) is obtained.

No shuffle is required in this transformation, meaning, the atoms remain in their crystallographic positions. The Bain correspondence, which related the fcc to bcc arrangement in metal structures, is now used to connect the anion arrangement in the spinel structure, which is approximately fcc, to the arrangements of anions in the Th_3P_4 structure, which is approximately bcc. It will turn out that some cations will undergo additional shuffle. This shuffle, however, is surprisingly small and corresponds only to a change in the coordination environment, but not to a significant diffusion. The transformation from spinel to Th_3P_4, or vice versa, will proceed through an energy barrier with height ΔE_a. Similar to conventional chemical kinetics, the rate of

transformation can now be described by an Arrhenius-type law. While the barrier must be overcome, the activation energy ΔE_a will correspond to a specific temperature. According to $T_a = \Delta E_a / K$ (or $T_a = \Delta E_a / R$, if one mole of particles is referenced). T_a is about the temperature at which the rate becomes significant. Depending on the direction of the process and the overall reaction enthalpy, T_a can be interpreted differently. If the reaction proceeds from a state with higher enthalpy to a state with lower enthalpy, T_a provides a measure for the (maximum) thermal stability of the initial state. If the initial and final state are equal in enthalpy, T_a may indicate the temperature above which equilibrium can be reached within a reasonable time.

3.2 Description of the structures: The spinel structure (fcc) and its bcc counterpart Th3P4 type

The spinel structure (A_2BX_4) adopts space group symmetry Fd-3m. In spinel the cations exist in two different environments: cations (A) in ½ of the octahedral sites and cations (B) in 1/8 of the tetrahedral sites. Anions are located in position 32e (x,x,x) with the free positional parameter $x = 3/8 + x_{sp}$. If $x_{sp} = 0$, the anions are at the points of a face centered cubic lattice (fcc). For all spinel structures the parameter x_{sp} is very close to zero. Note that the spinel structure has two parameters only: the lattice parameter and the positional parameter of the anions.

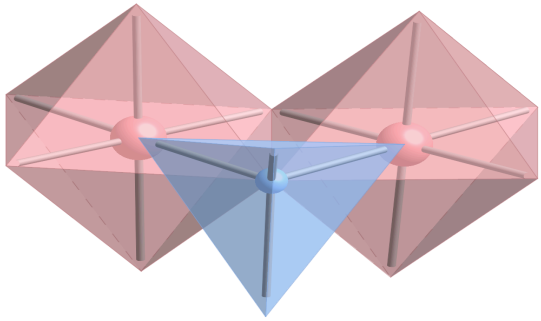

Figure 3: Spinel structure

The Th_3P_4 structure (A_3X_4) adopts space group symmetry I-43d [OKE96]. Cations (A) fill sites in 12a and anions (X) fill sites in 16c (x_b, x_b, x_b). Similar to the spinel structure, the Th_3P_4 structure

has only two parameters: the lattice parameter and the positional parameter of the anions. With x_b=0, the anion structure becomes ideal bcc. In the Th_3P_4-type, x_b is close to -1/12. In this case, the coordination polyhedron around each cation is a bisdisphenoid. This 8-fold coordination is composed of two interpenetrating tetrahedral, one stretched and the other one flattened. Anions are coordinated 6-fold in Th_3P_4 and the environment is described by a metaprism, which is between a trigonal prism and a trigonal anti-prism which ideally equals an octahedron.

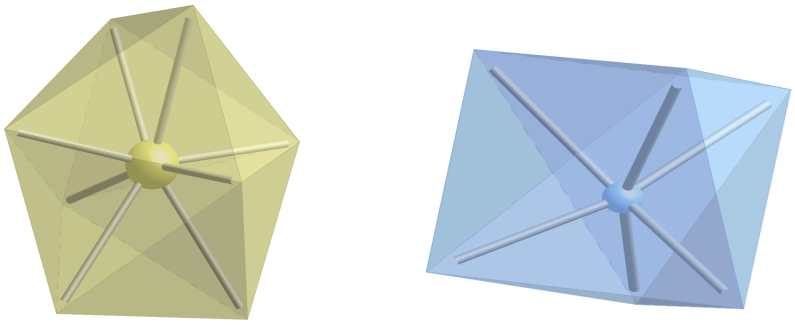

Figure 4: Th_3P_4 structure. (left) cation position, $\{A\}X_8$-bisdisphenoids and (right) anion position, $\{X\}A_6$-metaprisms

3.3 Crystallographic description of the transformation path

As pointed out before, spinel and Th_3P_4 structures adopt Fd-3m and I-43d space group symmetries respectively. To describe a path between the two structures, we choose the sub-group/ super-group approach. A common sub-group for both structures is I-42d. Description of these two structures using subgroup I-42d is given below:

Table 1: Crystallographic description of the transformation path

Spinel					Th_3P_4		
$a=a_{sp}$, $c/a=\sqrt{2}$					$a=c=a_b$		
Atom	Wy	x	y	z	x	y	z
A	4a	0	0	0	0	0	0
B	8d	½	¼	1/8	5/8	¼	1/8
X	16e	0	$¼-2x_{sp}$	$3/8+ x_{sp}$	x_b	$¼+2x_b$	$3/8+ x_b$

Here, a_{sp} and a_b are lattice parameters of spinel and Th_3P_4 respectively, and x_{sp} and x_b are the anion positional parameter of the conventional settings of spinel and Th_3P_4 structures, respectively. Wy stands for Wyckoff position.

Inspecting the table above, one observes that the cations in A position remain in their sites. Cation in B position change only in their x-coordinate. Anions change x, y, and z. However, given the fact that the anion structure parameter of spinel and Th_3P_4 , x_{sp} and x_b , are of small values, their move is very limited. Thus, as in the standard Bain transformation, the dominant change in structure is made by varying the lattice parameter a and changing the ratio c/a. Overall, we have 6 parameters to describe the transition. However, exploring the complete 6-dimensional potential energy (or enthalpy) surface is impossible.

As an approximation of the transformation path, a one-dimensional reaction coordinate has been constructed applying linear interpolation of all structural parameters. Static calculation performed on the intermediate structures yield an activation barrier, ΔE_a. Next, we did calculations at the transition pressure, which yields the temperature of synthesis for this phase transformation.

CHAPTER 4

RESULTS

4.1 Variation of energy and enthalpy under pressure

All hard materials, including diamond and c-BN, derived at high pressure are metastable at ambient pressure. These materials can withstand high temperatures during compaction treatments necessary to form a tool from the powdery source material as well as during actual performance as a tool. Therefore, the importance of high “metastability” or thermal stability cannot be ignored. The term thermal stability refers to the temperature at which decomposition or back transformation to the low-pressure polymorphs occurs [SCH03]. In order to access thermal stability (our first goal, as stated before), we need to follow a definite regime as stated previously in section 2.2.

First, taking the internal energy E as a function of the volume V for both Hf_3N_4 and Ti_3N_4 energy-volume (E-V) diagrams are constructed, considering three structure types –spinel, Th_3P_4 and lowest energy form o-Zr_3N_4 (in case of Hf_3N_4) and $CaTi_2O_4$ (for Ti_3N_4) in each case. Next, enthalpy difference-pressure (dH-p) diagrams constructed for Hf_3N_4 and Ti_3N_4 with reference to lowest energy state. The dH-p diagrams for Hf_3N_4 and Ti_3N_4 shows that, cubic Th_3P_4 will be adopted at high pressures, although it will be metastable at 0 GPa. Also from the diagram, the synthesized cubic Hf_3N_4 is a metastable compound having appreciable difference in energy (0.5 eV/f.u.) to the lowest energy Zr_3N_4-type (not yet synthesized) modification of Hf_3N_4. Spinel phase is metastable for any pressure-temperature condition. Similarly, cubic Ti_3N_4 (yet to synthesized) is a metastable compound with energy difference ~0.75 eV/f.u. to the lowest energy $CaTi_2O_4$-type (also not yet synthesized) [KRO04]. Also from the diagrams, the spinel modification is always lower than Th_3P_4 in energy but close to the Zr_3N_4 type at zero pressure, and is unfavorable towards compression at high pressure. For spinel -> Th_3P_4 type phase

transitions the transition pressures calculated are 3.9 and 4.9 for Hf_3N_4 and Ti_3N_4 respectively. Cubic Hf_3N_4 was synthesized around 18 GPa and can be quenched to 0 GPa. Thus, it may be possible to attain a phase that is thermodynamically metastable at zero pressure. If we can provide the temperature corresponding to spinel -> Th_3P_4 transition pressure (which was 3.9 and 4.87 for Hf_3N_4 and Ti_3N_4 respectively), it is possible to attain the spinel structure type on quenching. We want to predict an estimate of that temperature in this work.

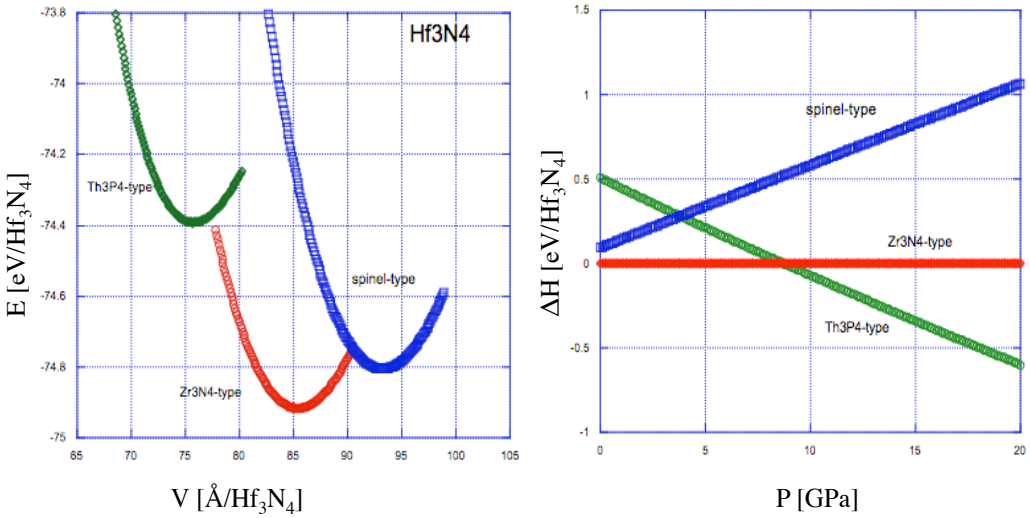

Figure 5: Energy-volume (E-V) (left) and enthalpy-pressure (ΔH-p) diagrams (right) of Hf_3N_4.

Table 2: Structure type, energy E_0 and volume V_0 calculated at zero pressure, relative energy ΔE with respect to the ground state configuration for the three polymorphs of interest of Hf_3N_4

Structure type	E_0	V_0	ΔE
o-Zr_3N_4	-74.908	85.28	0
Th_3P_4	-74.392	75.66	0.516
Spinel	-74.806	93.15	0.102

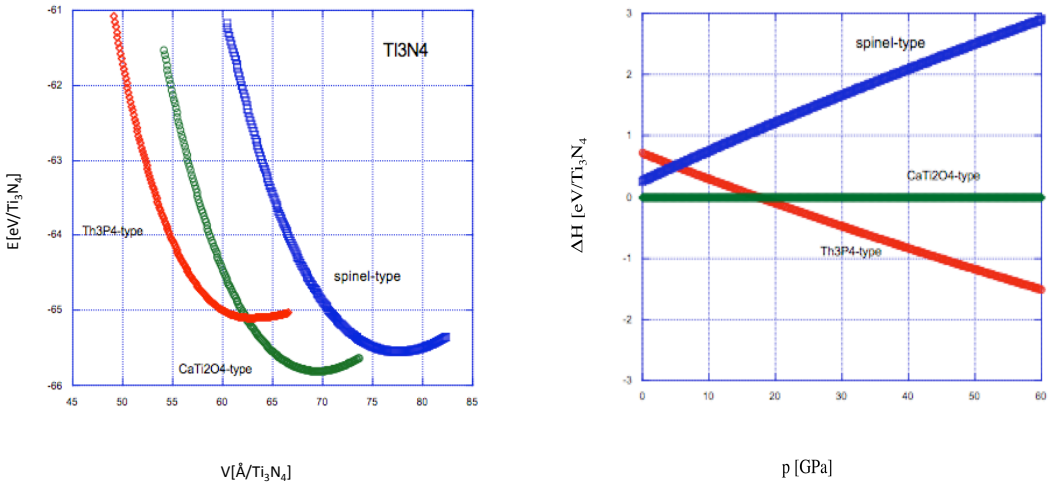

Figure 6: Energy-volume (E-V) (left) and enthalpy-pressure (ΔH-p) diagrams (right) of Ti_3N_4.

Table 3: Structure type, energy E_0 and volume V_0 calculated at zero pressure, relative energy ΔE with respect to the ground state configuration for the three polymorphs of interest of Ti_3N_4

Structure type	E_0	V_0	ΔE
$CaTi_2O_4$	-65.804	69.41	0
Th_3P_4	-65.097	62.75	0.707
Spinel	-65.550	77.56	0.254

4.2 Energy profile calculation along the reaction coordinate

A transformation scheme between spinel and Th_3P_4 retaining the symmetry of their common subgroup I-42d, was given at table 1 (page 13) before. As it implies, the transformation can be defined within six-dimensional configuration space as there are six parameters, which are changing during the transformation. A reaction coordinate was constructed by simultaneous linear interpolation of all the six structural parameters. Static calculations of these intermediate geometries yield an upper boundary of the activation barrier. The results of these calculations for Hf_3N_4 are shown below. The same regime was followed for Ti_3N_4 too.

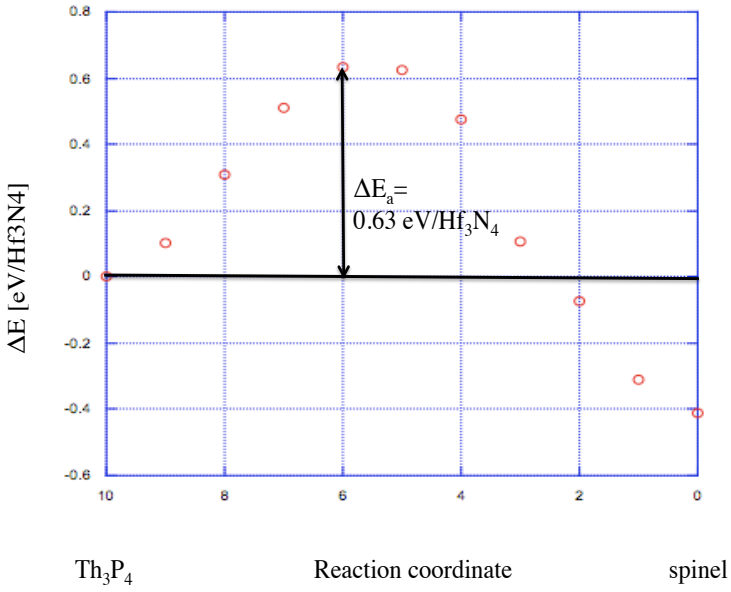

Figure 7: Energy profile diagram along the reaction coordinate for Hf_3N_4 (at 0 GPa). The linear interpolation was done for 9 points between Hf_3N_4 with spinel and Th_3P_4 structure types. All the six parameters were interpolated simultaneously. The activation energy Ea is about 0.63 eV per Hf_3N_4, the excess energy is equal to the energy difference between the spinel and the Th_3P_4 structure types, 0.4 eV per Hf_3N_4. In the x-axis 0 represents the spinel type while 10 is the Th_3P_4 type. (same notation is followed in the subsequent graphs).

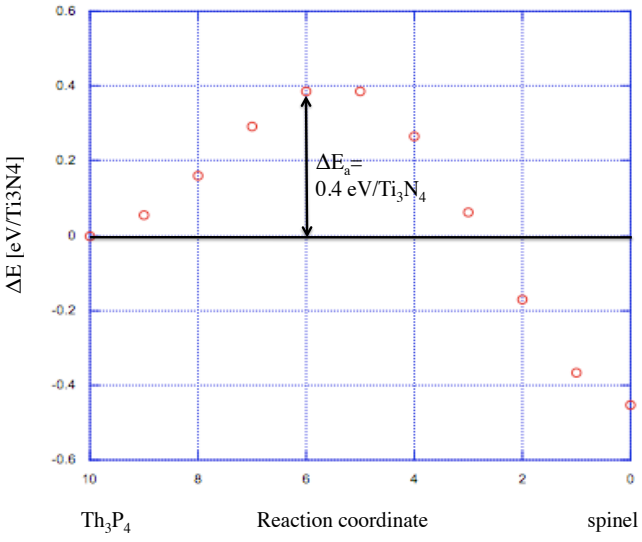

Figure 8: Energy profile diagram along the reaction coordinate for Ti_3N_4 (at 0 GPa). (Followed the same procedure as for Hf_3N_4). Here, the activation energy Ea is about 0.4 eV per Ti_3N_4, the

excess energy is equal to the energy difference between the spinel and the Th_3P_4 structure types, 0.48 eV per Ti_3N_4.

4.2.1 Results of energy profile calculation

Activation barrier can be calculated along a continuous path following a continuous path of structural transformation [figure 6 and 7]. From these static energy profile calculations at 0 GPa, barriers of 0.63 eV/f.u. and 0.4 eV/f.u. were estimated for the spinel->Th_3P_4 transformation for Hf_3N_4 and Ti_3N_4 respectively. On translating these energies per atom into temperature it gives 1125 K and around 800 K for Hf_3N_4 and Ti_3N_4 respectively, which corresponds to the thermal barrier. On comparing to typical bond-energies necessary to break during a reconstructive process of Hf-N and Ti-N bonds, these are significantly smaller barriers.

Now to achieve our second goal, that is to estimate the temperature of synthesis of still hypothetical spinel modification from cubic Th_3P_4 type on quenching, linear interpolation were done at the transition pressure (same procedure as before but previous calculations were done at 0 GPa). The results of these calculations are shown below:

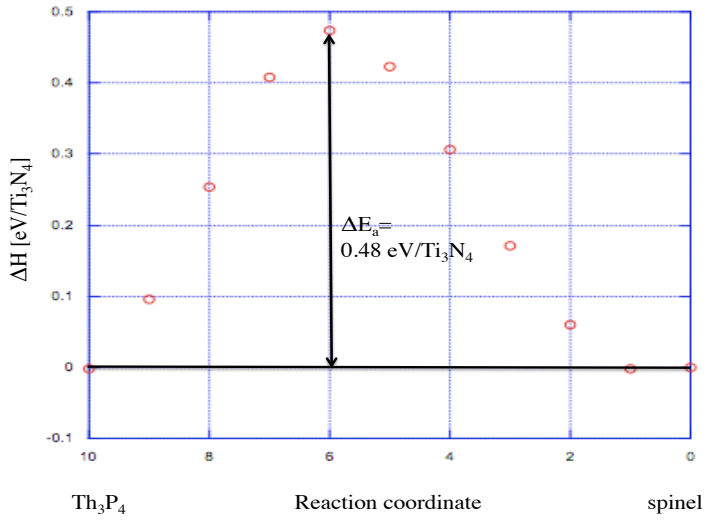

Figure 9: Enthalpy profile diagram along the reaction coordinate for Ti_3N_4. Calculations were done at transition pressure (P_t=4.9 GPa).

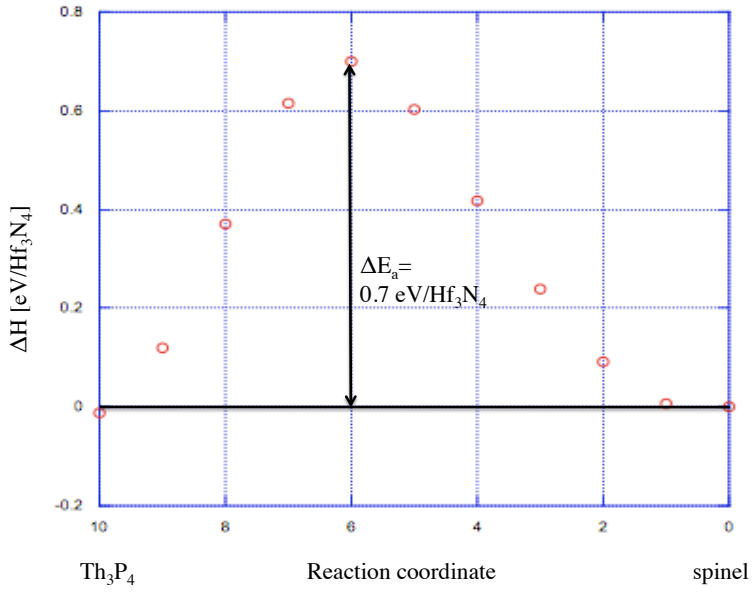

Figure 10: Enthalpy profile diagram along the reaction coordinate for Hf_3N_4 (P_t=4.9 GPa).

The same formalism was applied as before and calculations were carried out for the transformation at the transition pressure to access the temperature of synthesis. Barriers of 0.7 eV/f.u. and 0.48 eV/f.u. were estimated for Hf_3N_4 and Ti_3N_4 respectively. These energies corresponds temperatures of around 1200 K and 900 K respectively.

CHAPTER 5

SUMMARY AND CONCLUSION

Before the start of our work, we had two goals in our mind. First, to estimate the thermal stability of quenched high-pressure structures of recently synthesized cubic Th_3P_4 type for group 4 transition metal nitrides, namely Hf_3N_4 and Ti_3N_4. Second, to construct a pathway to synthesize novel structures, in our case, spinel phase. We concluded from our work that the spinel structure type may become accessible for group 4 transition metal nitrides Hf_3N_4 and Ti_3N_4.The Bain transformation path can be utilized to obtain the metastable spinel modification from Th_3P_4 by a kinetically activated process. At zero pressure where the spinel modification is energetically more favorable than the Th_3P_4 modification, the activation barrier fro spinel-> Th_3P_4 for Hf_3N_4 and Ti_3N_4 were found out to be 0.63 eV/f.u. and 0.4 eV/f.u. respectively. Hence, at temperatures around 1120 and 800 K this transformation will play a significant role on the decomposition of Hf_3N_4 and Ti_3N_4. Also we constructed the enthalpy profile diagram at the transition pressures and the barriers were found out to be 0.7 eV/f.u. and 0.48 eV/f.u. for Hf_3N_4 and Ti_3N_4 respectively. Hence, on providing temperatures 1200 K and 900 K to cubic Hf_3N_4 and Ti_3N_4, on quenching, the spinel modification can be attained.

REFERENCES

1. [AND97] Andrievski, R. A., “Films of interstitial phases: synthesis and properties”, J. Mater. Sci. 32, 4463 (1997)
2. [BOL09] Boldyreva, E., “High pressure crystallography: from fundamental phenomena to technological applications”, pp. 1-10 (Springer 2009).
3. [CHH05] Chhowalla, M. & H. E. Unalan, “Thin films of hard cubic Zr_3N_4 stabilized by stress”, Nat. Mater. 4, 317 (2005).
4. [CUE03] Cuevas, J., “Introduction to Density Functional Theory”, School on “Dynamics of interacting electrons in quantum wires”, Miraflores (Spain), 29 September - 4 October (2003).
5. [DZI09] Dzivenko, D., “High pressure synthesis, structure and properties of cubic zirconium (IV)- and hafnium (IV) nitrides.” Thesis, Darmstadt 2009.
6. [HOH64] Hohenberg, P., “Inhomogeneous electron gas.” Phys. Rev. 136, B864 (1964).
7. [HOR06] Horvath-Bordon, E. et al., “High pressure chemistry of nitride-based materials.” Chem. Soc. Rev., 2006, 35, 987-1014.
8. [KIB07] Kibey, S., “Mesoscale models for stacking faults, deformation twins and martensitic transformations: linking atomistics to continuum. Thesis, Urbana-Champaign 2007.
9. [KOH65] Kohn, W., “Self consistent equations including exchange and correlation effects.” Phys. Rev. 140, A1133 (1965)
10. [KOS01] Kostorz, G., “Phase transformations in materials”, pp. 1-80 (WILEY-VCH, Weinheim, 2001).
11. [KRA98] Kral, C., W. Lengauer, D. Rafaja & P. Ettmayer, “Critical review on the elastic properties of transition metal carbides, nitrides and carbonitrides”, J. Alloys Compd. 265, 215 (1998).
12. [KRE93] Kresse, G. et. al, ”Ab initio molecular dynamics for liquid metals.” Phys. Rev. B 47, 558 (1993).
13. [KRE96] Kresse, G. et. al, “Efficient iterative schemes for ab initio total-energy calculations using a plane-wave basis set.” Phys. Rev. B 54, 11169 (1996).
14. [KRE99] Kresse, G. et. al, “From ultrasoft pseudopotentials to the projector augmented-wave method.” Phys. Rev. B. 59, 1758 (1999)
15. [KRO03a] Kroll, P., “Pathways to metastable nitride structures.” Journal of Solid State Chemistry 176 (2003) 530-537.
16. [KRO03b] Kroll, P. “Hafnium nitride with thorium phosphide structure: physical properties and an assessment of the Hf-N, Zr-N, and Ti-N phase diagrams at high pressures and temperatures.” Physical Review Letters 90 (2003)
17. [KRO04] Kroll, P. “Assessment of the Hf-N, Zr-N and Ti-N phase diagrams at high pressures and temperatures: balancing between MN and M_3N_4 (M= Hf, Zr, Ti).” J. Phys.: Condens. Matter 16 (2004) S1235-S1244.
18. [LEN00] Lengauer, W., “Transition Metal Carbides, Nitrides, and Carbonitrides” in Handbook of Ceramic Hard Materials (ed. Riedel, R.), pp. 202-252 (WILEY-VCH, Weinheim, 2000).
19. [LER96] Lerch, M., E. Füglein & J. Wrba, “Synthesis, crystal structure, and high temperature behavior of Zr3N4”, Z. Anorg. Allg. Chem. 622, 367 (1996)
20. [LER97] Lerch, M., “Neue Anionendefizit-Materialen auf der Basis von ZrO_2: Synthese, Charakterisierung und Eigenschaften von ternären und quaternären Nitridoxiden des Zirconiums”, Postdoctoral thesis (Fakultät für Chemie und Pharmazie, Bayerische Julius-

Maximilians-Universität, Würzburg, 1997).
21. [MON07] Martinez, J., “Ab-initio study on synthesis of new materials at high pressure.” Thesis, SISSA 2007
22. [MUL06] Muller, U.,”Inorganic structural chemistry.” Second edition. John Wiley and sons Ltd. Chp. 4, 14, 17
23. [OKE96] O’Keeffe, M., “Crystal structures. I. Patterns and symmetry” (Mineralogical Society of America, Washington, D.C., 1996), p. 237f.
24. [SCH03] Schwarz, M., “High pressure synthesis of novel hard materials: spinel-Si_3N_4 and derivates. Thesis. Darmstadt 2003.
25. [YAO08] Yao, Y., “Structures, bonding and transport properties of high pressure solids.” Thesis. Saskatchewan 2008
26. [ZER99] Zerr, A. et. al. “Synthesis of cubic silicon nitride.” Nature 400 340-342 (July 1999)
27. [ZER03] Zerr, A. et al. ”Synthesis of cubic Zirconium and Hafnium nitride having Th_3P_4 structure.” Nature Materials 2003 March; 2, 185-189

BIOGRAPHICAL INFORMATION

Arindom Goswami was born in Assam, India on 1st of August 1984. He obtained his Bachelor's Degree in Chemistry from Jorhat Science College (now known as Jorhat Institute of Science and Technology) under Dibrugarh University, Assam India in 2006 August. Then, he completed his Master's Degree in Physical Chemistry from University of Delhi in July 2008. After showing immense interest in research, he joined The University of Texas at Arlington in fall 2009 and joined Dr. Peter Kroll's computational laboratory for pursuing research in the fields of nanosciences, ceramics and solid-state chemistry. It is the ultimate aim of his life to contribute to the field of Nanotechnology by doing cutting-edge research.